

## Theoretical insights of magnetizability and solvent effect on the electronic properties of $\text{CoB}_8^-$ molecule

Reza Ghiasi<sup>\*a</sup>, Amir Hossein Hakimoun<sup>b</sup>

<sup>a</sup>Department of chemistry, East Tehran Branch, Islamic Azad University, Qiam Dasht, Tehran, Iran

<sup>b</sup>Young Researchers and Elites club, North Tehran Branch, Islamic Azad University, Tehran, Iran

Received: 10 June 2015, Accepted: 30 April 2016, Published: 30 April 2016

### Abstract

Equilibrium geometry, electronic structures, and vibrational modes of  $\text{CoB}_8^-$  were investigated in the PBEPBE/6-311+G(d,p) level of theory. The nucleus independent chemical shift (NICS) analysis and magnetizability values were used for studying of aromaticity in  $\text{CoB}_8^-$ . The effects of different solvents on the structure and frontier orbital energies were calculated using the polarizable continuum model (PCM).  $\Delta E_{\text{solv}}$  values reveal increasing of stability in more polar solvents. Quantum theory of atoms in molecules (QTAIM) was used for the analysis of Co-B and BB bonds. This analysis shows the strong covalent and closed-shell interactions for B-B and Co-B bonds, respectively.

**Keywords:** Boron wheel molecules; solvent effect; magnetizability; QTAIM analysis; molecular orbital analysis.

### Introduction

The negatively charged boron clusters ( $\text{B}_n^-$ ) which possess planar (2D) structures at least up to  $n=23$  have been studied theoretically and experimentally [1-6]. Also, aromatic borometallic compounds, containing a highly coordinated central transition metal atom inside a monocyclic boron ring have been investigated. The stability of the  $\text{D}_{nh}\text{-M@B}_n^{k-}$  type molecular wheels and the prediction of new stable clusters have been rationalized (the “@” designates the central position of the doped atom in monocyclic structures) [7-9]. Theoretically investigations showed that the double aromatic character in chemical bonding was responsible for

their planarity and thus confirmed the wheel geometry of the B8 cluster [10].

The aromatic metal centered monocyclic boron rings  $\text{CoB}_8^-$  ( $\text{D}_{8h}$ ;  $^1\text{A}_{1g}$ ) have been detected experimentally [11]. The experimental results showed that shape of the anionic and neutral clusters are planar with a slight distortion, and the distances from the metal center to the boron and between the peripheral boron atoms were found to be 2.033 and 1.556 Å, respectively.

The current paper is computational study of solvent effect on the electronic properties of  $\text{CoB}_8^-$ . Also, a QTAIM-based Approach toward deciphering magnetic aromaticity has been used.

\*Corresponding author: Reza Ghiasi

Tel: +98 (912) 5330852, Fax: +98 (21) 33594337

E-mail: rezaghiasi1353@yahoo.com

### Computational method

All calculations were carried out with the Gaussian 09 suite of program [12]. The calculations were described by the standard 6-311+G(d,p) basis set [13-15]. Geometry optimization was performed using Perdew, Burke and Ernzerhof exchange functional [16, 17] and the gradient-corrected correlation functional of Perdew, Burke and Ernzerhof (PBE/PBE), and frequency calculation is done to confirm the status of the potential energy minimum.

Then the geometry of each species in solvents with different dielectric constants was calculated at the same level with the polarized continuum model (PCM) [18].

The nucleus-independent chemical shift (NICS) index, based on the magnetic criterion of aromaticity, is probably the most widely used probe for examination of chemical compounds aromatic properties [19]. It is defined as the negative value of the absolute magnetic shielding. It can be calculated in the centre of the aromatic ring (NICS(0) [20]), or at 1 Å above it (NICS(1) [21]). Negative NICS values denote efficient electron delocalization.

Nucleus-independent chemical shifts were calculated in the point located by 1 Å above the center of the ring (NICS(1)<sub>zz</sub>) as it was recommended for obtaining more accurate data [22, 23]. NICS values are calculated using the Gauge independent atomic orbital (GIAO) [24] method at the same method and basis sets for optimization.

The AIM2000 program [25] was used for topological analysis of electron density. The following characteristics of ring critical points (RCPs) are taken

into account: density at RCP ( $\rho(\text{rc})$ ), its Laplacian ( $\nabla^2\rho(\text{rc})$ ).

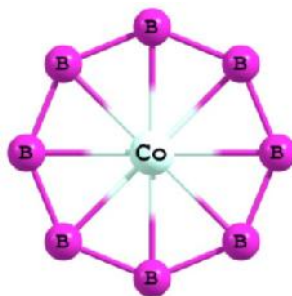
Intra- and interatomic magnetizabilities within the context of quantum theory of atoms in molecules (QTAIM)[26-29] were computed for the DFT-based electron densities. All magnetizability computations were performed employing the Proaim integration method, as implemented in the AIMAll suite of programs [30].

### Results and discussion

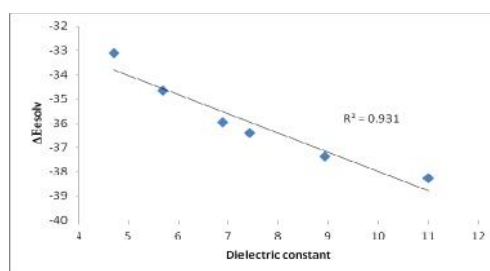
#### Energy

Figure 1 presents the molecular structure of  $\text{Co}@\text{B}_8^-$  molecule. The energies of  $\text{Co}@\text{B}_8^-$  molecule in gas phase and in different media using the polarizable continuum model (PCM) model are gathered in Table 1.  $E_T$  is the total energy and  $\Delta E_{\text{solv}}$  is the stabilization energy of solvents, ie the relative energy of the title compound in a solvent to that in the gas phase.

From Table 1, we can see that the calculated energy is dependent on the magnitude of the dielectric constant of solvents. In the PCM model, the energies  $E_T$  decrease with the increasing dielectric constants of solvents. On the other hand,  $\Delta E_{\text{solv}}$  values indicate the increasing of stability in more polar solvents. This is because a dipole in the molecule will induce a dipole in the medium, and the electric field applied to the solute by the solvent (reaction) dipole will in turn interact with the molecular dipole to lead to net stabilization. This suggests that the  $\text{Co}@\text{B}_8^-$  molecule has more stability in polar solvent rather than in the gas phase. There is a good correlation between dielectric constants and  $\Delta E_{\text{solv}}$  (Figure 2).



**Figure 1.** The structure of  $\text{Co@B}_8^-$  molecule



**Figure 2.** The correlation between dielectric constants and  $\Delta E_{\text{solv}}$  in  $\text{Co@B}_8^-$  molecule

**Table 1.** Absolute energy ( $E_T$ , Hartree), solvation energy ( $E_{\text{solv}}$ , kcal/mol), solvent dielectric constant ( $\epsilon$ ), BB and CoB bond lengths (in Å) of  $\text{Co@B}_8^-$  molecule in the PBE/PBE/6-311+g(d,p) level of theory

$\text{Co@B}_8^-$	$\epsilon$	$E_T$	$E_{\text{solv}}$	$r(\text{BB})$	$r(\text{Co-B})$
<b>Gas</b>	-	-1580.9896	-	1.5692	2.0502
<b>Chloroform</b>	4.71	-1581.0424	-33.11	1.5678	2.0485
<b>chlorobenzene</b>	5.70	-1581.0449	-34.67	1.5678	2.0483
<b>Aniline</b>	6.89	-1581.0469	-35.96	1.5677	2.0483
<b>THF</b>	7.43	-1581.0476	-36.41	1.5677	2.0483
<b>methylenechloride</b>	8.93	-1581.0492	-37.38	1.5677	2.0483
<b>isoquinoline</b>	11.00	-1581.0506	-38.28	1.5676	2.0483

#### Bond distances

The bond distances of  $\text{Co@B}_8^-$  molecule have been collected in Table 1. It is well-known that the solvent polarity influences both the structure and properties of conjugated organic

molecules and metal complexes [31-33]. The structural data for the optimized structures of  $\text{Co@B}_8^-$  molecule in the six studied solvents are gathered in Table 1. The results show that the structural parameters are

changed by the polarity of the surrounding media. These values indicate shortening of Co–B and lengthening of BB bonds in the set of solvents rather than gas phase.

#### Vibrational spectral analysis

A vibrational analysis of IR active vibrational modes has been reported on the basis of DFT/B3LYP/6-

311++G(d,p) quantum chemical calculations. The calculated vibrational wavenumbers and vibrational modes are presented in Figure 3. The most intensity vibrational mode is attributed to the out-of-plane modes in  $52.1 \text{ cm}^{-1}$ . The other observed strong bands in  $439.4$  and  $842.5 \text{ cm}^{-1}$  are assigned to ring asymmetric deformation modes.

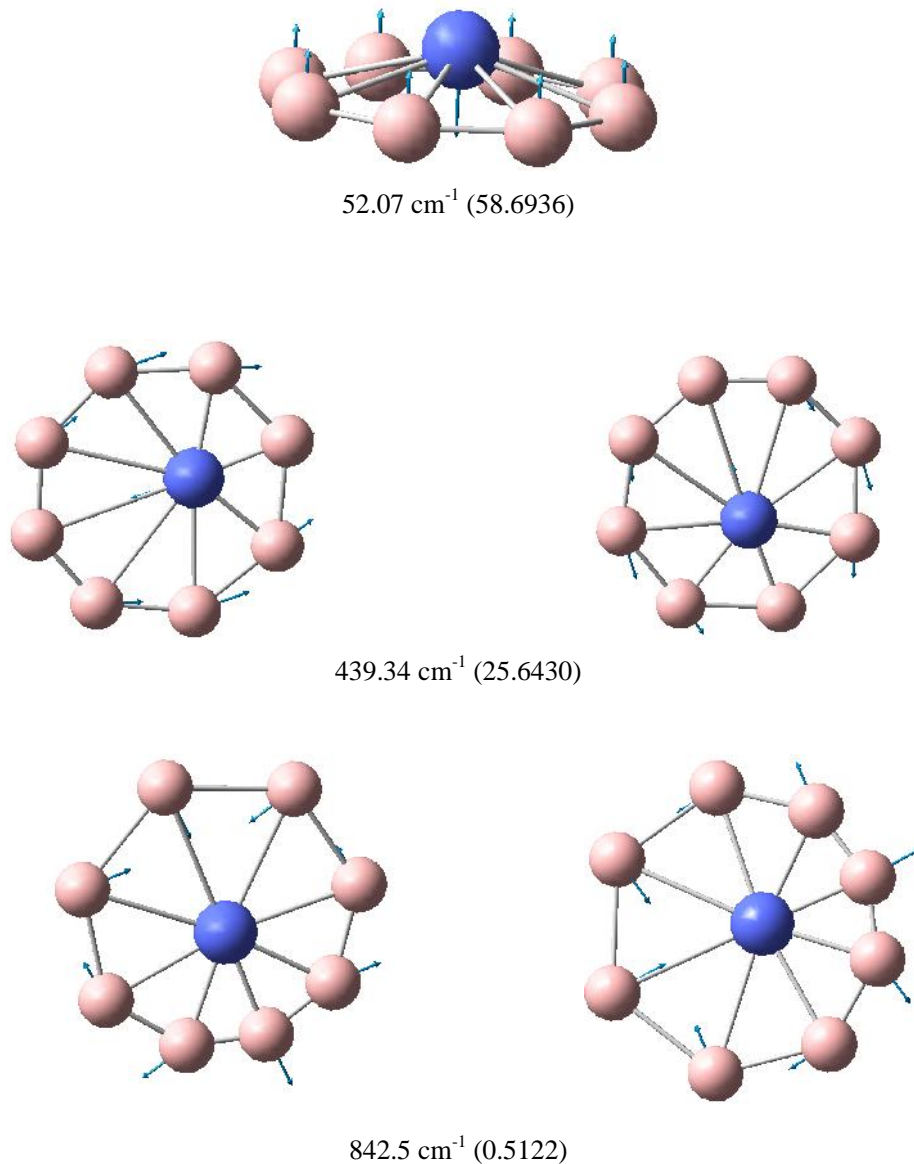


**Figure 3.** The wave number, intensity (in parenthesis), and vibrational modes of IR active vibrational in  $\text{Co@B}_8$  molecule

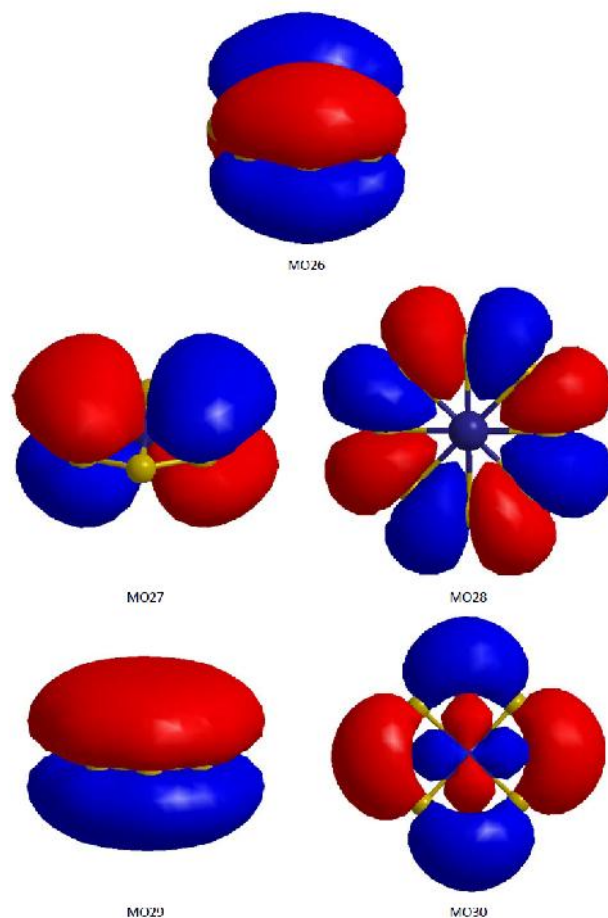
### Molecular orbital analysis

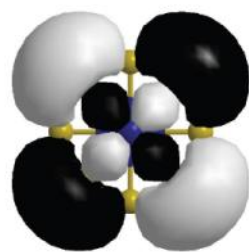
The energies of the frontier orbitals (HOMO, LUMO) along with the corresponding HOMO–LUMO energy gaps, Hardness, chemical potential, and electrophilicity of  $\text{Co}^{\ominus}\text{B}_8$  molecule are gathered in Table 2. Frontier orbital analysis presents the HOMO and LUMO which are not distributed on nitrogen atom (Figure 4). The HOMO of  $\text{Co}^{\ominus}\text{B}_8$  molecule is at  $-0.05265$  Hartree while its LUMO is at  $-0.00650$  Hartree as calculated. This yields an HOMO–LUMO energy gap of  $1.256$  eV. The HOMO–LUMO gap values are in the typical magnitude (i.e., less than  $2$  eV) of semiconductors [34]. Therefore, it could be expected that this molecule might be considered as the

novel building blocks in practical applications.

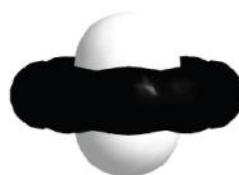
Inclusion of solvation effects leads also to changes on the molecular orbital energies (Table 2). In solution, HOMO and LUMO energies are stabilized, with respect to the corresponding values in vacuum. On the other hand, frontier orbitals energies in various solvents show the increasing stability of these orbitals in more polar solvents. Figure 5 presents good linear correlations between dielectric constant and frontier orbitals energies.

The comparison of HOMO-LUMO gaps in different solvents show the increasing of this value in more polar solvents.

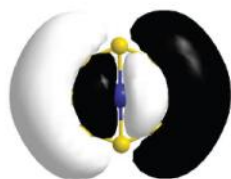




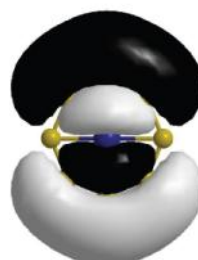
M031



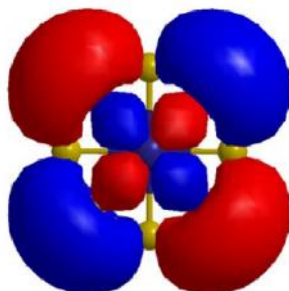
M032



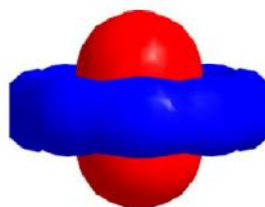
M033



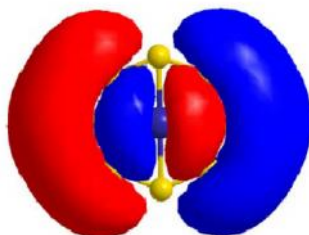
M034



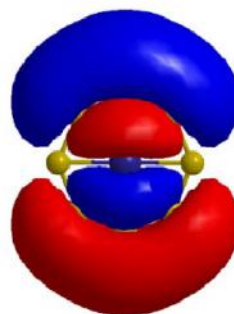
M031



M032



M033



M034

**Figure 4.** The selected molecular orbital of Co@B<sub>8</sub><sup>-</sup> molecule

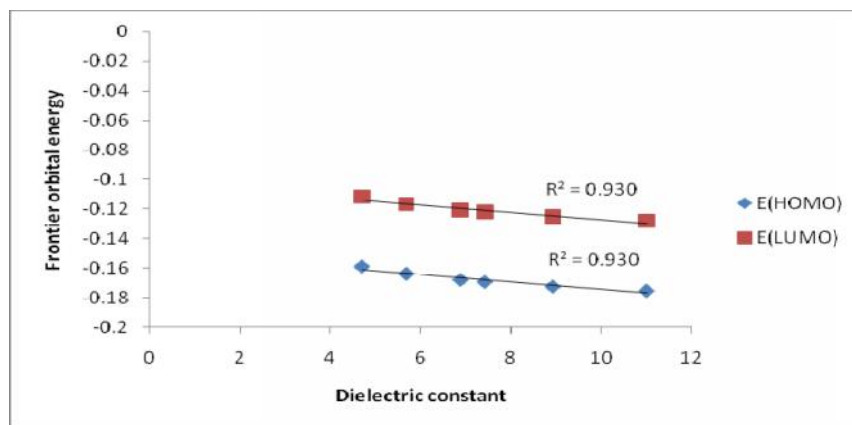


**Figure 5.** Correlations between dielectric constant and frontier orbitals energies in  $\text{Co@B}_8^-$  molecule

**Table 2.** The frontier orbital energies (Hartree), HOMO-LUMO gap (eV), hardness (eV), chemical potential (eV), and electrophilicity (eV) of  $\text{Co@B}_8^-$  molecule in gas and solution phases

$\text{Co@B}_8^-$	E(HOMO)	E(LUMO)	UE	$\chi$	$\eta$	$\omega$
Gas	-0.05265	-0.00650	1.256	0.628	-0.805	0.516
Chloroform	-0.15856	-0.11170	1.275	0.638	-3.677	10.604
chlorobenzene	-0.16352	-0.11661	1.276	0.638	-3.811	11.380
aniline	-0.16763	-0.12066	1.278	0.639	-3.922	12.037
THF	-0.16905	-0.12206	1.279	0.639	-3.961	12.269
methylenechloride	-0.17212	-0.12509	1.280	0.640	-4.044	12.778
isoquinoline	-0.17497	-0.12790	1.281	0.640	-4.121	13.258

### NICS values

The nucleus-independent chemical shift (NICS) index, based on the magnetic criterion of aromaticity, is probably the most widely used probe for examination of chemical compounds aromatic properties [19]. It is defined as the negative value of the absolute magnetic shielding. NICS values are calculated using the Gauge independent atomic orbital (GIAO) [24] method at the same method and basis sets for optimization.

Table 3 encloses the values corresponding to NICS aromaticity criteria [35]. NICS values have been calculated in center and 0.5, 1.0, 1.5, 2.0, 2.5 and 3.0 Å above of the center of triangle rings. Figure 6 and Table 3 indicate the most negative NICS values 1.0 Å above of the rings center are compatible with  $\pi$ -aromaticity of  $\text{Co@B}_8^-$  ring. On the other hand, NICS<sub>zz</sub> scan show the most negative NICS values in the center of rings. Therefore, NICS(0.0)<sub>zz</sub> values results to a pure  $\pi$ -ring current.

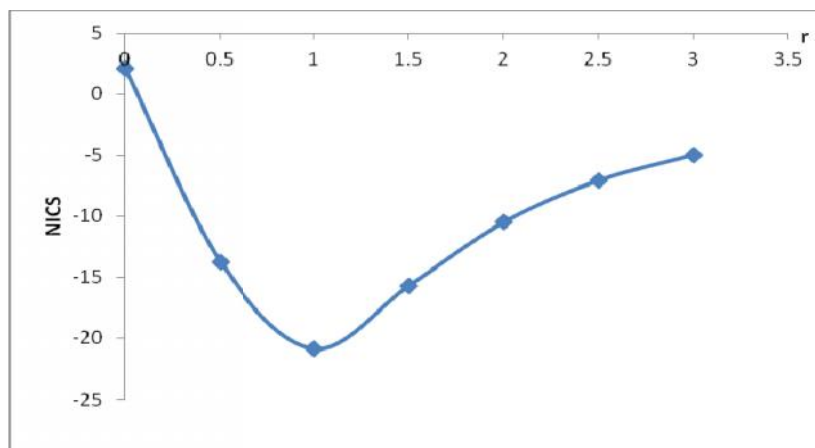


**Figure 6.** Profile of variation of NICS values with distance from the center of triangle rings of  $\text{Co@B}_8^-$  molecule

**Table 3.** Nucleus-independent chemical shift (NICS) values of  $\text{Co@B}_8^-$  molecule

r	0.0	0.5	1.0	1.5	2.0	2.5	3.0
NICS	2.11	-13.75	-20.88	-15.72	-10.50	-7.07	-4.96
NICS <sub>zz</sub>	-52.43	-44.38	-33.44	-24.99	-18.39	-13.48	-9.96

#### Quantum theory of atoms in molecules analysis (QTAIM)

As shown in Table 4, different values of electron density for B-B and Co-B bonds clearly indicate the B-B stronger bonds.

In the case of all the Co-B bonds,  $\nabla^2\rho$  values at corresponding BCPs are positive, as it was found for closed-shell interactions, but the value of  $H(\rho)$  is negative, as found for shared

interactions. This is in agreement with observations made for the M-C bonds in organometallic complexes [36, 37], in this sense the metal-ligand bonding has a characteristic that represents a mix of the closed-shell and shared parameters. In the B-B bonds  $\nabla^2\rho$  and  $H(\rho)$  values at corresponding BCPs are negative, as it was found for strong covalent interactions.

**Table 4.** Electron densities  $\rho$  ( $e/a_0^3$ ), Laplacians  $\nabla^2\rho$  ( $e/a_0^5$ ), total electron energy density,  $H(\rho)$ , kinetic energy density,  $G(\rho)$ , and potential energy density,  $V(\rho)$  at critical points for  $\text{Co@B}_8^-$  molecule

	$\rho$	$\nabla^2\rho$	$G(\dots)$	$H(\dots)$	$V(\dots)$
<b>Co-B</b>	0.0930	0.1390	0.0682	-0.0334	-0.1016
<b>B-B</b>	0.1686	-0.3712	0.0428	-0.1356	-0.1785

#### Magnetizability

Intra- and interatomic magnetizabilities as well as their out-of-plane components, which are in particular associated with the ring currents, are useful for studying of aromaticity [38].

The small, negative  $\chi_{zz}(\text{Co})$  and  $\chi_{zz}(\text{B})$  values indicate the presence of weak local electronic currents (Table 5). Negative atomic magnetizabilities denote the presence of net local diatropic currents. On the other hand,

based on the values of  $t_{zz}(\text{Co|B})$ , and  $t_{zz}(\text{B|B})$ , we can consider this cluster as a magnetically aromatic compound (Table 6). Negative bond magnetizabilities denote aromatic character. Investigating the contributions of individual MOs, obtained within the context of DFT, in the atomic and interatomic magnetizabilities demonstrates that MO28 and MO25 for BB bonds, and MO33, MO34, MO28, MO27, MO26, MO24, and MO23 among the valence molecular orbitals for CoB, sustain diatropic currents, whereas the rest of the valence MOs are paratropic; the MOs are depicted in Figure 4. The  $\pi$ -type MO28 of the  $\text{Co@B}_8^-$  molecule is responsible for  $\sim 68\%$  of the out-of-

plane bond magnetizability of  $\text{B}_B$  bond. On the other hand, the degenerate  $\pi$ -type MO23, and MO24 of the  $\text{Co@B}_8^-$  molecule are responsible for 98% of the out-of-plane bond magnetizability of CoB bond i.e. magnetic aromaticity. The  $\pi$ -type MO26 and MO27 of the  $\text{Co@B}_8^-$  molecule are responsible for  $\sim 47.5\%$  of the out-of-plane bond magnetizability of CoB bond. It is worth mentioning that individual  $\pi$ -type MOs do not contribute considerably to the bond magnetizability of BB bonds; but, contribute considerably to the bond magnetizability of CoB bonds. Indeed, the molecule generally benefits from  $\pi$ ,  $\pi$ -aromaticity in the context of magnetic aromaticity.

**Table 5.** Isotropic and out of plane intra-atomic magnetizabilities of  $\text{Co@B}_8^-$  in cgs-ppm units at the PBE/PBE/6-311+g(d,p) level of theory for  $\text{Co@B}_8^-$  molecule

$\text{Co@B}_8^-$	$t(\text{Co})$	$t(\text{B})$	$t_{zz}(\text{Co})$	$t_{zz}(\text{B})$
<b>total</b>	42.339	0.270	-13.511	-2.072
<b>MO33,34</b>	-3.3393	2.0074	-3.2756	5.3605
<b>MO32</b>	-8.7454	0.8404	20.5609	-18.4603
<b>MO30,31</b>	-25.0577	-1.2566	-11.4690	20.9536
<b>MO29</b>	2.0317	0.7139	0.1428	0.2591
<b>MO28</b>	-0.0892	-1.9244	-0.1782	-3.7760
<b>MO26,27</b>	-0.0312	0.7271	2.3553	0.1694
<b>MO25</b>	-11.5709	-0.2040	0.8201	1.6108
<b>MO23,24</b>	-0.1348	-1.6915	-0.1828	-1.9209
<b>MO22,21</b>	-0.5045	0.2220	-2.6449	-0.2500
<b>MO20,19</b>	-0.2783	-0.0806	1.2250	-1.8024
<b>MO18</b>	0.0340	0.1432	0.7705	-0.3045
<b>Core</b>	90.0246	0.7727	-21.6356	-3.9116

**Table 6.** Isotropic and out of plane inter-atomic magnetizabilities of  $\text{Co}@\text{B}_8\text{B}_8$  in cgs–ppm units at the PBEPBE/6-311+g(d,p) level of theory for  $\text{Co}@\text{B}_8$  molecule

$\text{Co}@\text{B}_8$	t ( $\text{B}^*\text{B}'$ )	t ( $\text{Co}^*\text{B}'$ )	t ( $_{zz}(\text{B}^*\text{B}')$ )	t ( $_{zz}(\text{Co}^*\text{B}')$ )
<b>total</b>	-2.2984	-2.0670	-5.4599	-4.9101
<b>MO33,34</b>	0.7536	-0.8029	2.1030	-1.3262
<b>MO32</b>	0.2420	0.4499	0.2488	0.4632
<b>MO30,31</b>	-0.5897	1.2069	-0.3520	3.5553
<b>MO29</b>	0.9343	0.5988	1.4514	0.9303
<b>MO28</b>	-1.3270	-1.1605	-3.7664	-3.1974
<b>MO26,27</b>	1.1077	-0.6512	2.4669	-2.3305
<b>MO25</b>	-0.1914	1.5291	-0.2981	4.4529
<b>MO23,24</b>	0.0525	-2.0409	0.3900	-4.8156
<b>MO22,21</b>	0.3252	1.9217	0.5024	4.3963
<b>MO20,19</b>	0.5738	0.4224	1.6424	1.2583
<b>MO18</b>	0.2972	0.2743	0.6964	0.5280
<b>Core</b>	-4.4764	-3.8147	-10.5447	-8.8246

### Conclusion

In this paper has been shown:

1. The study of solvent effect on the  $\text{Co}@\text{B}_8$  molecule illustrated decreasing of solvent energies  $E_T$  and increasing of  $\Delta E_{\text{solv}}$  values with the increasing dielectric constants of solvents, respectively.
2. In the basis of molecular orbital analysis, HOMO and LUMO energies stabilized in solution, with respect to the corresponding values in vacuum. Also, frontier orbitals energies in various solvents show the increasing stability of these orbitals in more polar solvents.
3. The most intensity vibrational modes are attributed to the out-of-plane and ring asymmetric deformation modes.
4. The most negative NICS values have been found at 1.0 Å above of the rings center are compatible with  $\pi$ -aromaticity in  $\text{Co}@\text{B}_8$  ring. On the other hand, the most negative NICS values are in the center of rings. Therefore,  $\text{NICS}(0.0)_{zz}$  values results to a pure  $\pi$ -ring current.

5. QTAIM analysis indicates strong covalent and closed-shell interactions for B–B and Co–B bonds, respectively.

6. The magnetizability values show that molecule usually benefits from  $\pi$ -aromaticity.

### Acknowledgements

The authors thank Dr. S. Jamehbozorgi, for helpful comments and valuable suggestions that helped the authors to improve the quality of this paper.

### References

- [1] H.J. Zhai, Alexandrova, A.N. Birch, K.A. Boldyrev, A.I. Wang, L.S. *Angew. Chem., Int. Ed.*, **2003**, *42*, 6004–6008.
- [2] H.J. Zhai, B. Kiran, J. Li, L. S. Wang, *Nat. Mater.*, **2003**, *2*, 827–833.
- [3] A.N. Alexandrova, H.J. Zhai, L.S. Wang, A.I. Boldyrev, *Inorg.Chem.*, **2004**, *43*, 3552–3554.
- [4] A.N. Alexandrova, A.I. Boldyrev, H.J. Zhai, L.S. Wang, *J. Phys. Chem. A.*, **2004**, *108*, 3509–3517.
- [5] B. Kiran, S. Bulusu, H.J. Zhai, S. Yoo, X.C. Zeng, L.S. Wang, *Proc. Natl. Acad. Sci. U.S.A.*, **2005**, *102*, 961–964.

- [6] A.N. Alexandrova, A.I. Boldyrev, H. J. Zhai, L.S. Wang, *Coord. Chem. Rev.*, **2006**, *250*, 2811–2866.
- [7] C. Romanescu, T.R. Li, W.-L. Galeev, A.I. Bpldyrev, L.-S. Wang, *Accounts of Chemical Research*, **2013**, *46*, 350–358.
- [8] L. Xie, W.-L. Li, C. Romanescu, X. Huang, L.-S. Wang, *Tje Journal of Chemical Physics*, **2013**, *138*, 034308-11
- [9] C. Romanescu, T.R. Galeev, W.-L. Li, A.I. Boldyrev, L.-S. Wang, **2013**, *138*, 134315-8.
- [10] P. Bonacic-Koutecký, J. Koutecký, *Chem. Rev.*, **1991**, *91*, 1035-1108.
- [11] C. Romanescu, T.R. Galeev, W.-L. Li, A.I. Boldyrev, L.-S. Wang, *Angew. Chem. Int. Ed.*, **2011**, *50*, 9334–9337.
- [12] M.J. Frisch, G.W. Trucks, H. B. Schlegel, G.E. Scuseria, M.A. Robb, J. R. Cheeseman, G. Scalmani, V. Barone, B. Mennucci, G. A. Petersson, H. Nakatsuji, M. Caricato, X. Li, H.P. Hratchian, A.F. Izmaylov, J. Bloino, G. Zheng, J.L. Sonnenberg, M. Hada, M. Ehara, K. Toyota, R. Fukuda, J. Hasegawa, M. Ishida, T. Nakajima, Y. Honda, O. Kitao, H. Nakai, T. Vreven, J.A.M. Jr., J.E. Peralta, F. Ogliaro, M. Bearpark, J.J. Heyd, E. Brothers, K.N. Kudin, V.N. Staroverov, T. Keith, R. Kobayashi, J. Normand, K. Raghavachari, A. Rendell, J.C. Burant, S.S. Iyengar, J. Tomas, M. Cossi, N. Rega, J.M. Millam, M. Klene, J.E. Knox, J.B. Cross, V. Bakken, C. Adamo, J. Jaramillo, R. Gomperts, R. E. Stratmann, O. Yazyev, A. J. Austin, R. Cammi, C. Pomelli, J.W. Ochterski, R.L. Martin, K. Morokuma, V.G. Zakrzewski, G.A. Voth, P. Salvador, J. J. Dannenberg, S. Dapprich, A.D. Daniels, O. Farkas, J.B. Foresman, J.V. Ortiz, J. Cioslowski, D.J. Fox, Gaussian 09, Revision B.01. Gaussian, Inc., Wallingford CT.
- [13] P.C. Hariharan, J. A. Pople, *Theo. Chim. Acta.*, **1973**, *28*, 213-222.
- [14] P. C. Hariharan; Pople, J. A.: *Mol. Phys* **1974**, *27*, 209-214.
- [15] M.J. Frisch, J.A. Pople, J.S. Binkley, *J. Chem. Phys.*, **1984**, *80*, 3265-3269.
- [16] P. Perdew, K. Burke, M. Ernzerhof, *Phys. Rev. Lett.*, **1996**, *77*, 3865-3868.
- [17] J.P. Perdew, K. Burke, M. Ernzerhof, *Phys. Rev. Lett.*, **1997**, *78*, 1396-1396.
- [18] J. Tomasi, B. Mennucci, R. Cammi, *Chem. Rev.*, **2005**, *105*, 2999-3093.
- [19] Z. Chen, C.S. Wannere, C. Corminboeuf, R. Puchta, P.V.R. Schleyer, *Chem. Rev.*, **2005**, *105*, 3842–3888.
- [20] P.V.R. Schleyer, C. Marker, A. Dransfeld, H. Jiao, N.J.R.V. Hommes, *J. Am. Chem. Soc.*, **1996**, *118*, 6317–6318.
- [21] P.V.R. Schleyer, M. Monohar, Z. Wang, B. Kiran, H. Jiao, R. Puchta, N. J.R.V. Hommes, *Org. Lett.*, **2001**, *3*, 2465–2468.
- [22] C. Corminboeuf, T. Heine, G. Seifert, P.V.R. Schleyer, J. Weber, *Phys. Chem. Chem. Phys.*, **2004**, *6*, 273–276.
- [23] H. Fallah-Bagher-Shaidaei, C.S. Wannere, C. Corminboeuf, R. Puchta, P.V.R. Schleyer, *Org. Lett.*, **2006**, *8*, 863–866.
- [24] K. Wolinski, J.F. Hinton, P. Pulay, *J. Am. Chem. Soc.*, **1990**, *112*, 8251–8260.
- [25] R.F.W. Bader, AIM2000 Program. ver 2.0, ed.: Hamilton, McMaster University, **2000**.
- [26] R.F.W. Bader, *In Atoms in Molecules: A Quantum Theory*; Oxford University Press: Oxford, **1990**.
- [27] T.A. Keith, R.F.W. Bader, *J. Chem. Phys.*, **1993**, *99*, 3669-3682.

- [28] T.A. Keith, R.F.W. Bader, *Chem. Phys. Lett.*, **1993**, *210*, 223-231.
- [29] T.A. Keith, *In The Quantum Theory of Atoms in Molecules: From Solid State to DNA and Drug Design*; Wiley-VCH: Weinheim, Germany, **2007**.
- [30] T. A. Keith, AIMAll 11.02.27 ed.; <http://aim.tkgristmill.com>.
- [31] P.J. Mendes, T.J.L. Silva, A.J.P. Carvalho, J.P.P. Ramalho, *Journal of Molecular Structure: THEOCHEM*, **2010**, *946*, 33-42.
- [32] L.M. Chen, J.C. Chen, H. Luo, al., e.: *Journal of Theoretical and Computational Chemistry* **2011**, *10*, 581-604.
- [33] X. Cao, C. Liu, Y. Liu, *Journal of Theoretical and Computational Chemistry*, **2012**, *11*, 573-586.
- [34] X.-J. Li; Su, K.-H.: *Theor Chem Acc* **2009**, *124*, 345-354.
- [35] Z. Chen, C.S., Wannere, C. Corminboeuf, R. Puchta, P.V.R. Schleyer, *Chem. Rev.*, **2005**, *105*, 3842-3888.
- [36] R.F.W. Bader, C.F. Matta, *Inorg. Chem.* **2001**, *40*, 5603-5611.
- [37] M. Palusiak, *J. Organomet. Chem.*, **2007**, *692*, 3866-3873.
- [38] I. Cernusak, P.W. Fowler, E. Steiner, *Mol. Phys.*, **2000**, *98*, 945-953.